

# An experimental and computational investigation of the standard temperature-pressure correction factor for ion chambers in kilovoltage x rays

Daniel J. La Russa<sup>a)</sup>

Carleton Laboratory for Radiotherapy Physics, Ottawa Carleton Institute of Physics, Carleton University, Ottawa, ON K1S 5B6, Canada

Malcolm McEwen

Ionizing Radiation Standards, National Research Council of Canada, M-35 Montreal Road, Ottawa, ON K1A 0R6, Canada

D. W. O. Rogers<sup>b)</sup>

Carleton Laboratory for Radiotherapy Physics, Ottawa Carleton Institute of Physics, Carleton University, Ottawa, ON K1S 5B6, Canada

(Received 8 June 2007; revised 22 August 2007; accepted for publication 24 September 2007; published 15 November 2007)

For ion chambers with cavities open to the surrounding atmosphere, the response measured at a given temperature and pressure must be corrected using the standard temperature-pressure correction factor ( $P_{TP}$ ). A previous paper based solely on Monte Carlo simulations [D. J. La Russa and D. W. O. Rogers, *Med. Phys.* **33**, 4590–4599 (2006)] pointed out the shortcomings of the  $P_{TP}$  correction factor when used to correct the response of non-air-equivalent chambers for low-energy x-ray beams. This work presents the results of several experiments that corroborate these calculations for a number of ion chambers. Monte Carlo simulations of the experimental setup revealed additional insight into the various factors affecting the extent of the breakdown of  $P_{TP}$ , including the effect of impurities and the sensitivity to chamber dimensions. For an unfiltered 60 kV beam, the  $P_{TP}$ -corrected response of an NE 2571 ion chamber measured at 0.7 atm was 2.5% below the response measured at reference conditions. In general, Monte Carlo simulations of the experimental setup using EGSnrc were within 0.5% of measured values. EGSnrc-calculated values of air kerma calibration coefficients ( $N_K$ ) at low x-ray energies are also provided as a means of estimating the level of impurities in the chambers investigated. Calculated values of  $N_K$  normalized to the value measured for a 250 kV beam were obtained for three chambers and were within 1% of experiment with one exception, the Exradin A12 in a 50 kV beam. © 2007 American Association of Physicists in Medicine. [DOI: 10.1118/1.2799580]

Key words: temperature-pressure correction, air pressure, ion chamber dosimetry, x ray, correction factors, Monte Carlo, EGSnrc

## I. INTRODUCTION

In a recent pair of papers,<sup>1,2</sup> the ADCL at the University of Wisconsin reported problems with the standard temperature-pressure correction factor ( $P_{TP}$ ) when used with well ionization chambers made of non-air-equivalent materials. The factors affecting the extent of the problem were established through a series of experiments, and confirmed with extensive Monte Carlo simulations. A follow-up investigation by our group<sup>3</sup> based on Monte Carlo calculations revealed similar problems with the  $P_{TP}$  correction factor when used to correct the response of various non-air-equivalent ion chambers in low-energy x-ray beams. The problems are more severe for large  $P_{TP}$  corrections despite the fact that the  $P_{TP}$  correction, given as

$$P_{TP} = \left( \frac{273.15 + T/^\circ\text{C}}{273.15 + T_0/^\circ\text{C}} \right) \left( \frac{P_0}{P} \right), \quad (1)$$

is routinely used at all air densities.<sup>3</sup> In the above relation,  $T$  and  $P$  are the temperature and pressure within the cavity in

units of °C and kPa, respectively, whereas  $T_0$  and  $P_0$  are, correspondingly, the reference temperature (22 °C in North America) and pressure (101.325 kPa).

Having identified the breakdown of the  $P_{TP}$  correction factor at low x-ray energies with Monte Carlo simulations, it is prudent to fully scope the effect experimentally. Experimental evidence has been reported previously in a publication written in German by Will and Rakow,<sup>4</sup> and later in internal reports at the National Physical Laboratory (NPL) by Burns and Pritchard<sup>5</sup> for an NE 2561 chamber (now NE 2611). The latter data were presented at a BIPM conference in 1977 and are still included in the instruction manual for each new NE 2611 chamber. However, not enough details of those experiments are reported to allow for accurate Monte Carlo modeling, and experimental data only exist for a handful of chambers. In this work, we present a more comprehensive set of experimental data confirming the breakdown of the  $P_{TP}$  correction factor at low energies for several commonly used ion chambers made with and without non-

TABLE I. Physical characteristics of the Farmer-type thimble ionization chambers as modeled in this investigation. The diameter of the electrodes are all 1.0 mm, including the Exradin A2 chambers which normally come with a 4.6 mm diameter electrode. In all cases, the wall thickness was sufficient to provide full buildup for each beam quality used in this investigation. The mean chord length,  $L$ , represents the average distance an electron must travel to cross the cavity, given by  $L=4V/S$ , where  $V$  is the volume of the cavity and  $S$  is the surface area. Radiographs and schematic diagrams of the NE 2571 and Exradin A12 chambers are given in Ref. 9, and the NE 2505/3 chambers were used in previous studies (Ref. 7).

Chamber	Wall		Electrode material	Nominal collecting volume (cm <sup>3</sup> )	$L=4V/S$ (cm)
	Material	Thickness (mm)			
NE 2571	Graphite	0.36	Aluminum	0.6	0.48
NE 2505/3 (modified)	Graphite	0.36	Aluminum	0.6	0.48
	Dural	0.09	Aluminum	0.7	0.52
Exradin A19	C-552	0.5	C-552	0.6	0.46
Exradin A12	C-552	0.5	C-552	0.6	0.54
Exradin A2 (modified)	C-552	1.0	C-552	0.7	1.24
	C-552	1.0	Aluminum	0.7	
	Aluminum	1.0	C-552	0.7	
	Aluminum	1.0	Aluminum	0.7	

air-equivalent materials. The results of these experiments are reproduced by Monte Carlo simulations of our experimental setup as a means of corroborating our previous calculations, and to demonstrate the efficacy of our Monte Carlo codes at low photon energies.

## II. METHODS AND PROCEDURES

### II.A. Ion chambers

The ion chambers used in this investigation are listed in Table I. Ignoring differences in guard design, the chambers studied may be grouped according to the geometrical configuration of the cavity; those having cavity dimensions similar to the NE 2571, and those similar to an Exradin A2 with a thin electrode (1.0 mm diameter). An Exradin A12 was also investigated due to its calibration history and familiarity in the laboratory. The chambers listed, although similar in dimension, are composed of various wall and electrode materials, thereby permitting an investigation into the respective influences of the materials on chamber response as a function of air density. Table I lists these materials for each chamber, along with the nominal collecting volume and mean chord length of the cavity,  $L$ , calculated using  $L=4V/S$  which holds rigorously for isotropic electrons incident on concave cavities.<sup>6</sup> To gauge the effect of impurities, the composition and impurity level of the dural (an aluminum alloy) and graphite NE 2505/3 thimbles were measured at NRC using x-ray fluorescence spectroscopy with an uncertainty of  $\pm 10\%$  on the impurities. Table II lists the results of this analysis. A description of the NE 2505/3 chambers is given in previous reports,<sup>7,8</sup> while radiographs and schematics of the NE 2571 and Exradin A12 chambers are provided by McCaffrey *et al.*<sup>9</sup>

### II.B. X-ray spectra and Monte Carlo simulations of the NRC x-ray tube

In all experimental measurements the Comet MXR-320 x-ray system at NRC was used as a source of x rays. Table III lists the beam qualities used when measuring the response as a function of air density [ $M(\rho)$ ] along with those used to obtain  $N_K$  values for three of the chambers. Spectral distributions of these beams were calculated using a BEAMnrc (Ref. 10) simulation of the x-ray source by combining the methods of Mainegra-Hing and Kawrakow,<sup>11</sup> and Ali and Rogers.<sup>12</sup> The calculated spectra were found to be nearly identical to the corresponding spectra in IPEM Report 78,<sup>13</sup> calculated using the method of Birch and Marshall<sup>14</sup> (data

TABLE II. Results of the x-ray fluorescence spectroscopy analysis of the graphite and dural thimbles for the NE 2505/3 chamber listed in Table I. The total of the respective fractions for dural did not equal 100% so the balance of the composition was taken as aluminum in our EGSnrc model.

Thimble	Material	Atomic number	% composition by weight
Graphite	Graphite	6	98.87
	Silicon	14	0.11
	Chlorine	17	0.43
	Calcium	20	0.59
Dural	Oxygen	8	2.40
	Magnesium	12	0.81
	Aluminum	13	90.14
	Silicon	14	0.49
	Manganese	25	0.73
	Iron	26	0.40
	Copper	29	4.58
Zinc	30	0.10	

TABLE III. X-ray beams used in the investigation. The half-value layer (HVL) is defined as the thickness of material (Al or Cu) required to reduce the measured air kerma to one-half of the original value at 1 m distance from the source. The calculated HVLs for the simulated spectra were determined using Eq. 12 of Ref. 11. The effective energies ( $E_{\text{eff}}$ ) in this case are defined as the energy of a monoenergetic photon beam having the same HVL as the corresponding spectrum.

For $N_K$ curves						
Tube kV	Filtration (mm)		HVL (mm)		$E_{\text{eff}}$ (keV)	
	Al	Cu	Experiment	Calculation	Experiment	Calculation
50	1.032	-	1.102 (Al)	1.048	22.74	22.63
60 <sup>a</sup>	1.032	-	1.209 (Al)	1.219	23.49	23.90
100	3.63	-	4.022 (Al)	4.038	37.09	38.16
135	1.00	0.25	0.488 (Cu)	0.461	59.96	58.86
180	1.25	0.50	0.991 (Cu)	0.940	79.55	77.66
250	1.00	1.70	2.533 (Cu)	2.414	122.52	122.11

For $M(\rho)$ vs $\rho$			
Tube kV	Filtration (mm)		Avg. calc. photon $E$
	Al	Cu	(keV)
60	-	-	22.9
100 <sup>b</sup>	3.63	-	50.9
150 <sup>c</sup>	1.00	0.246	70.0
150	1.00	0.495	76.0

<sup>a</sup>Only used for the calibration of the NE 2571.

<sup>b</sup>Only used with the Exradin A12.

<sup>c</sup>Only used with the NE 2571.

not shown). Half-value layers (HVL) of the calculated spectra used to obtain calibration coefficients were determined using Eq. 12 of Ref. 11, and were found to be within 5.5% of experimental values. This agreement is within the range reported in previous studies,<sup>15–17</sup> and confirms that the x-ray source was well modeled. Values of air kerma per unit fluence ( $K_{\text{air}}$ ) for each of the x-ray spectra used were calculated using the EGSnrc “g” user-code.

### II.C. Experimental measurements

The ability of the  $P_{TP}$  correction factor to correct the response of each of the chambers listed in Table I was tested by measuring as a function of pressure the response of the chamber placed within an air-tight vessel made of polymethylmethacrylate (PMMA). A diagram of the experimental setup is shown in Fig. 1. The PMMA vessel is cylindrically symmetric with an outer diameter of approximately 30 cm and a wall thickness of 0.65 cm. The air pressure within the vessel, and therefore in the cavity of the chambers, was reduced using a vacuum pump, and monitored using a high-precision electronic barometer which was regularly calibrated against a secondary standard pressure meter throughout the course of these experiments. The temperature within the vessel was monitored using a platinum sensor connected to an external DMM via a vacuum-sealed feed-through. An additional feed-through connected the ion chamber to a Keithley 6517A electrometer which controlled the bias and measured the ionization. The ion chambers were positioned with their cavities centered in the field of view

and supported in the vessel by an aluminum stand outside of the field. The field size at 100 cm from the source was collimated to a diameter of 9 cm, and the distance between the source and the axis of symmetry of the chamber was  $123 \pm 1$  cm.

Before each data set was acquired, the ion chamber in the vessel was pre-irradiated until a stable reading was reached relative to the monitor chamber.<sup>9</sup> All ion chamber measurements were computer-controlled with a collection time cho-

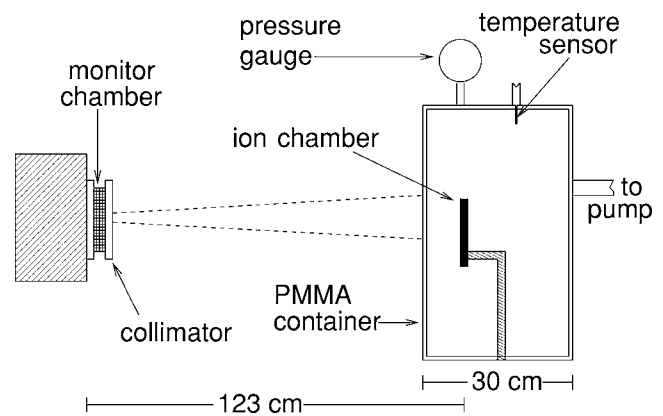


FIG. 1. Schematic of the experimental setup. The ion chambers were supported by an aluminum stand within a cylindrical PMMA vessel (0.65 cm thick walls) and laser-aligned in the center of the field. The field size was collimated to a diameter of 9 cm at a distance of 100 cm. Note that the diagram is not drawn to scale, and the x-ray tube and monitor chamber are only shown for perspective.

TABLE IV. Estimated uncertainties associated with the experimentally measured chamber response per unit response of the monitor chamber.

Component	Std. unc. (%)	Comment
Type A:		
Repeatability—short term	0.03	Standard deviation of the mean of 7–10 readings once stable reading was reached
Pressure correction—zero offset	0.04	Based on calibrations with reference pressure gauge
Pressure correction—linearity	0.08	Based on calibrations with reference pressure gauge
Type B:		
Temperature stability	0.01	Analysis assumed constant $T$ . Uncertainty estimated from experimental data as temperature stabilized after pressure change.
Reference pressure gauge	0.02	From uncertainty in calibration
Humidity	0.05	Not monitored inside vessel
Hysteresis of pressure change	0.05	Estimated from repeated measurements after changing pressure
Drift of system	0.08	Could be chamber, x-ray tube, or monitor chamber (pre-irradiation effects considered)
Overall:	0.14	Consistent with long term repeatability (between independent measurements)

sen according to the magnitude of the signal (between 10 and 60 s), and the electrometers were rezeroed between successive charge measurements. The air pressure in the vessel was then reduced and varied at random to values as low as 0.5 atm (i.e., measurements were not obtained in order of decreasing air pressure). At each pressure, the chamber was allowed to stabilize, which also provided enough time for the temperature to re-equilibrate after cooling/heating upon adiabatic expansion/compression. The measured response was then taken as the average of the last seven to ten stable charge measurements by the chamber divided by the charge measured by the monitor chamber, with a standard deviation of the mean of 0.03% or less. Measurements at atmospheric pressure were repeated after the pressure in the vessel had been ramped in order to confirm that hysteresis effects were negligible. Uncertainties on these measurements were estimated using the ISO Guide to the Expression of Uncertainty in Measurement,<sup>18,19</sup> and are summarized in Table IV. Air kerma calibration coefficients ( $N_K$ ) for three of the chambers were also obtained for x-ray beams listed in the top part of Table III following the standard calibration procedures at NRC.

#### II.D. Monte Carlo calculations of ion chamber response

Calculations of ion chamber response were performed with the EGSnrc Monte Carlo computer code system for coupled transport of charged particles and photons.<sup>20–22</sup> With the exception of the values used with the variance reduction techniques, the EGSnrc parameters used in these simulations were the same as those reported in a previous paper.<sup>3</sup> The “cavity” user-code, based upon a C++ geometry package,<sup>23</sup> was used to model the vessel and ion chamber shown in Fig. 1 since it provided the flexibility necessary to simulate complex geometrical configurations. Thus, to the best of our

knowledge, the dimensions and physical shape of the chambers were modeled exactly as specified by the manufacturers, including the cone-shaped tops of the NE-type chambers, and the hemispherical tops of the Exradin A12 and Exradin A2 chambers. Using the spectra calculated from the above-mentioned BEAMnrc simulation as a source, the calculated dose to the cavity ( $D_{cav}$ ) at an air density  $\rho$  was assumed to be proportional to the response,  $M(\rho)$ , corrected by  $P_{TP}$ . This assumption was justified in a preceding paper,<sup>3</sup> and in related reports by Bohm *et al.*<sup>2</sup> and Griffin *et al.*<sup>1</sup>

In order to simulate changes in air pressure within the PMMA vessel and chamber cavities, interaction cross sections for air were generated for a variety of air densities. This was done merely for convenience since EGSnrc does not, in general, require separate cross-section data sets for different densities of the same material unless changes in the density effect are important. The reference air density corresponding to  $T_0$  and  $P_0$  [Eq. (1)] was taken as 1.196 kg/m<sup>3</sup>, and humidity effects were taken into account by slightly adjusting the fractions of atomic components to give 50% relative humidity, which is consistent with the relative humidity measured throughout the course of the experiments. The relative amounts of each element in humid air for this humidity level were interpolated from the data in Table XIV of the AAPM TG-43 update.<sup>24</sup> This level of humidity reduces the reference air density by about 0.5%, but the change was ignored since it was found that the effect on the calculated results was completely negligible for small changes in  $\rho_0$ . In our preceding paper,  $\rho_0$  was set to 1.205 kg/m<sup>3</sup>, which corresponds to the density of air at a temperature of 20 °C at the same reference pressure, and thus represents the value of  $\rho_0$  for Europe. In North America,  $\rho_0$  is 0.7% lower but the difference in values has a negligible effect on the calculations we reported previously since they are normalized relative to  $\rho_0$ .

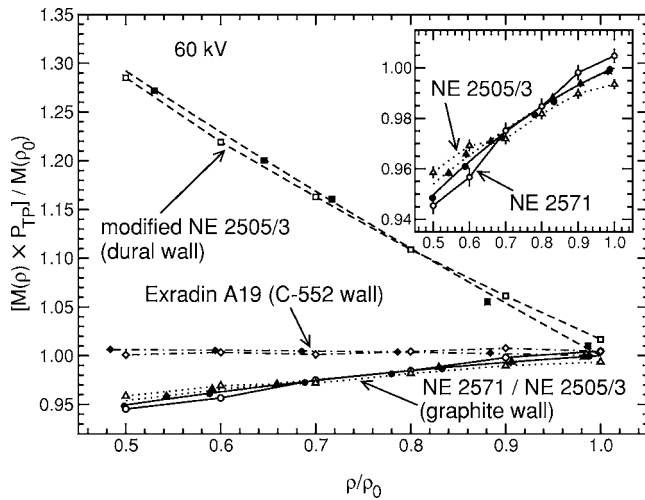


FIG. 2. Measured and calculated responses due to the unfiltered 60 kV beam as a function of air density for the NE 2571, Exradin A19, and NE 2505/3 chambers enclosed in the PMMA vessel (Fig. 1).  $P_{TP}$ -corrected measurements (closed symbols) were fit to second-order polynomials which were then normalized to unity at the reference air density ( $\rho_0$ ). Calculated values of chamber response (open symbols) were normalized to the fit line for each chamber using the method of least squares. The NE 2505/3 chambers were modeled using the composition of the wall measured with x-ray fluorescence spectroscopy (Table II). The NE 2571 and Exradin A19 were modeled with no impurities. All statistical uncertainties on the calculations are 0.35% or less.

### III. RESULTS

#### III.A. NE 2571-type chambers

Measured and EGSnrc-calculated responses of the NE 2571, Exradin A19, and NE 2505/3 chambers as a function of pressure due to the unfiltered 60 kV beam (Table III) are shown in Fig. 2. The measured responses (closed symbols) were corrected by the standard  $P_{TP}$  correction factor [Eq. (1)] using our measurements of temperature and pressure within the vessel. These data were then fit to a second-order polynomial using the method of least squares, and the fit lines were normalized to unity at the air density corresponding to reference temperature and pressure conditions ( $1.196 \text{ kg/m}^3$ ). The second-order term in the polynomials acted only as a smoothing term, and the coefficients were typically an order of magnitude less than the slope (i.e., measured data sets are approximately linear). Calculated responses (open symbols), which inherently include the  $P_{TP}$  correction, were normalized to the fit of the corresponding measurements so as to minimize the difference between the calculated and measured values. The data were compared in this way since normalizing to the calculated response at  $\rho_0$  could give a misleading comparison due to the statistical fluctuations in the calculated results. Thus, no emphasis is given to any one calculated value. Furthermore, a comparison of this type avoids fits of the calculated data to an arbitrary function, which would be subject to the larger relative statistical fluctuations and therefore difficult to visually interpret.

Prior to preceding reports,<sup>1-5</sup> no variation in ion chamber response was expected as a function of air density in the

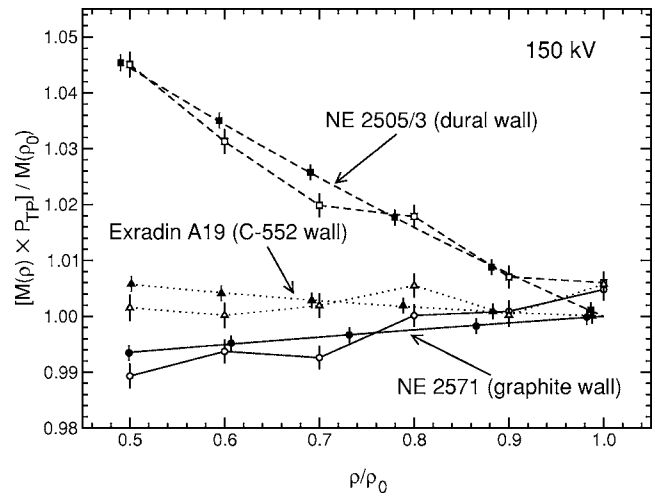


FIG. 3. As in Fig. 2 except for the 150 kV beam, with the range of the ordinate significantly reduced. The more softly filtered 150 kV beam was used with the NE 2571 chamber (Table III). Statistical uncertainties on the calculations are approximately 0.2%.

cavity if the deviations in temperature and pressure from reference conditions were accounted for by the  $P_{TP}$  correction factor. The variations in the calculated and measured,  $P_{TP}$ -corrected responses shown in Fig. 2 therefore reveal a shortcoming in the  $P_{TP}$  correction factor used with the unfiltered 60 kV beam incident on three of the four chambers. The corrected response measured for the modified NE 2505/3 chamber with dural walls deviated above the normalized response by over 13% at an air density typical for Mexico City ( $\rho/\rho_0=0.76$ ). The normal configuration of the NE 2505/3 with graphite walls deviated below the normalized response by 2% at the same air density, as did the response of the NE 2571. These measured data are corroborated by Monte Carlo calculations, which matched the corresponding measured data sets to within 1.5% for the dural NE 2505/3, and to within 0.5% for the other chambers. The graphite NE 2505/3 and the NE 2571 have nearly identical dimensions and chamber materials, but the EGSnrc model of the NE 2505/3 included the impurities in the wall that were measured using x-ray fluorescence spectroscopy (Table II), whereas the model of the NE 2571 had walls of pure graphite. The inset of Fig. 2 shows that the Monte Carlo results were able to track the differences in the respective responses due to the presence of impurities. The photon cross sections of pure graphite are less than air, and so the presence of high-Z impurities makes the graphite thimble of the NE 2505/3 slightly more air-equivalent. As a result, the variation in the measured and calculated  $P_{TP}$ -corrected response of this chamber is less than that of the NE 2571. Finally, measured and calculated data for the Exradin A19 with air-equivalent walls and electrode were constant within 1% over the whole range of air densities tested, indicating that the  $P_{TP}$  correction factor is reliable for chambers made of air-equivalent walls.

Measurements and calculations of the response of these chambers repeated in the 150 kV beam are shown in Fig. 3.

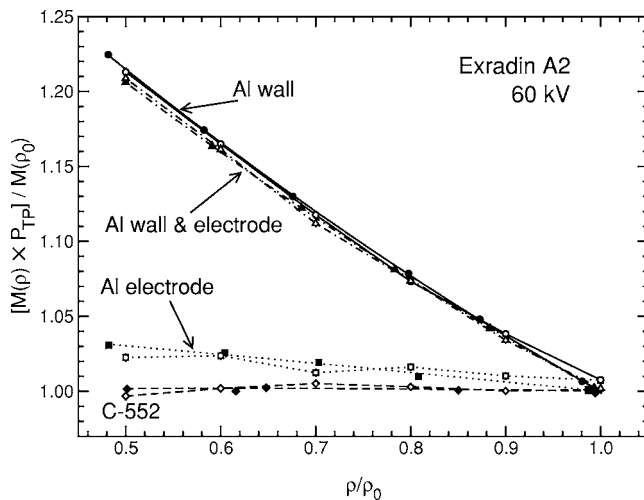


FIG. 4. As in Fig. 2 but for the modified Exradin A2 chambers. Experimental results are indicated by closed symbols, and the corresponding EGSnrc calculations by open symbols. The dashed line shows results for an Exradin A2 made with C-552 air-equivalent plastic walls and electrode. The dotted line shows results for an otherwise identical chamber with an aluminum electrode of the same thickness (1 mm). Results for these same two chambers with an aluminum thimble replacing the C-552 plastic walls are shown in the solid lines and dotted-dashed lines, respectively. Statistical uncertainties on the calculations are 0.3% or less.

Overall, the variation in the measured and calculated  $P_{TP}$ -corrected responses is significantly less than the 60 kV beam case, with variations within 1% of the normalized response for the NE 2571 and the Exradin A19 chambers. This is consistent with previous findings based on EGSnrc calculations.<sup>3</sup> In this study, the EGSnrc-calculated response of these two chambers matched experimental values to within 0.5%. Data for the graphite-walled NE 2505/3 differed negligibly from those for the NE 2571, and so were not included here. The measured and calculated responses of the modified NE 2505/3 chamber with dural walls deviated 4.5% above the normalized response over the range of air densities tested.

### III.B. Modified Exradin A2 chambers

The breakdown of the  $P_{TP}$  correction factor is also demonstrated by the data presented in Figs. 4 and 5 for the modified Exradin A2 chambers. The experimental data were analyzed in the same manner as described for the NE-type chambers. For the 60 kV beam case (Fig. 4) at  $\rho/\rho_0=0.5$ , measurements and calculations of the  $P_{TP}$ -corrected response of this chamber with aluminum walls deviate by over 20% above the normalized response. Including an aluminum electrode with the Al-walled chamber configuration had a negligible effect on this variation. For the completely air-equivalent chamber made of C-552 plastic, no variation was observed within 0.5%. However, the chamber with C-552 air-equivalent plastic walls and an aluminum electrode produced a 3% variation in the  $P_{TP}$ -corrected response over the range of air densities tested.

Figure 5 shows data for the same chambers as in Fig. 4, but for the 150 kV beam. The overall variation in the nor-

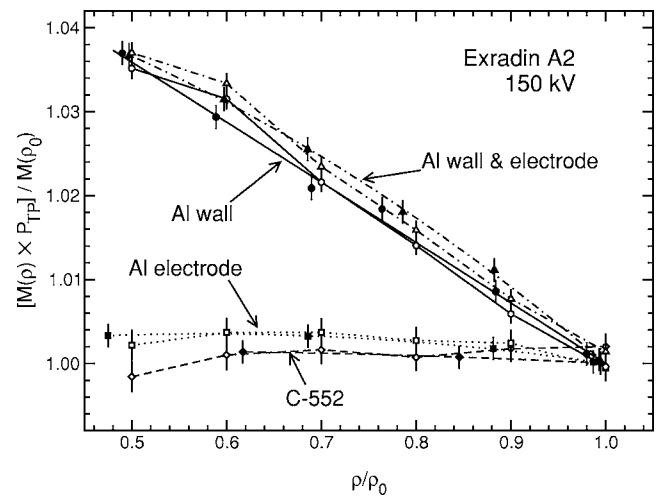


FIG. 5. As in Fig. 2 for the modified Exradin A2 chambers and the 150 kV beam. As is the case for the NE type chambers, the scale of the ordinate is significantly reduced relative to the corresponding data for the unfiltered 60 kV beam (Fig. 4). Statistical uncertainties on the calculations are approximately 0.35%.

malized, corrected response observed with the aluminum-walled chambers is less than 4%. A relatively small variation (<0.5%) was observed for the chambers with air-equivalent walls, both with and without the aluminum electrode.

### III.C. Exradin A12 chamber and calculations of $N_K$

Measurements and calculations of the Exradin A12 for the 100 kV (Table III) and unfiltered 60 kV beams incident on the Exradin A12 chamber are shown in Fig. 6. Unlike the other air-equivalent chambers, an unexpected 1.6% variation in the measured,  $P_{TP}$ -corrected response was observed with

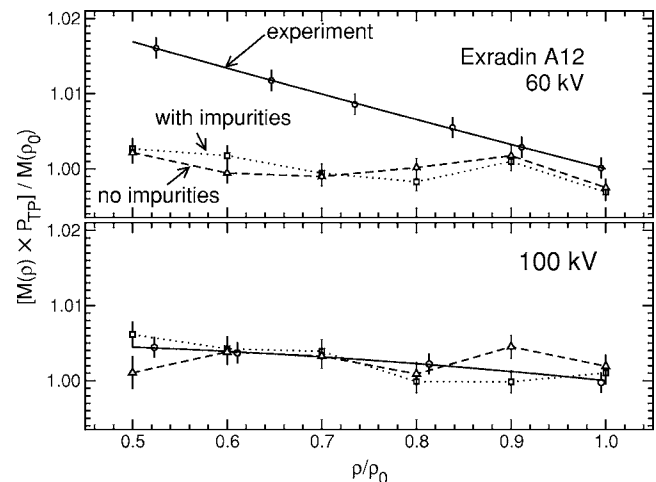


FIG. 6. As in Fig. 2 for the 100 kV and unfiltered 60 kV beams incident on Exradin A12 chamber enclosed in the PMMA vessel.  $P_{TP}$ -corrected responses were calculated with (dotted line) and without (dashed line) the addition of high-Z impurities in the C-552 plastic. Since calculations of response for the 60 kV beam case did not reflect the variation observed experimentally, the data were collectively normalized to unity in order to make differences in the respective trends easier to visualize. The calculated responses for the 100 kV beam were normalized to the experimental data as in Fig. 2. All statistical uncertainties on the calculations are 0.3% or less.

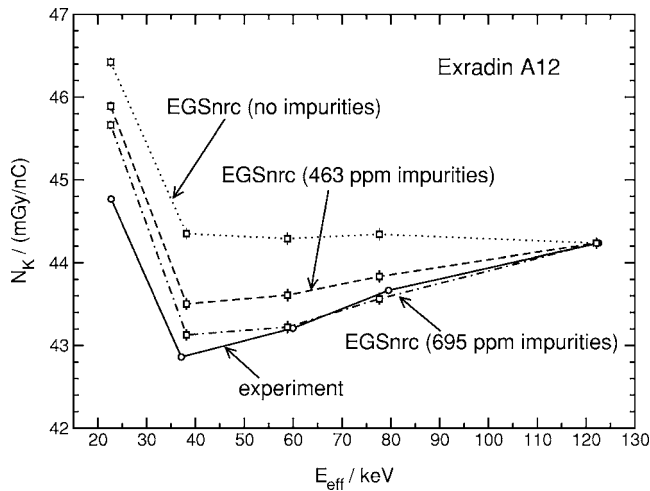


FIG. 7. Measured and EGSnrc-calculated air kerma calibration coefficients as a function of beam effective energy for the Exradin A12 chamber used in this study.  $N_K$  values were calculated for the chamber simulated with (dotted line) and without (dashed lines) high- $Z$  impurities in the C-552 plastic walls, and normalized to the experimental value corresponding to the 250 kV beam ( $E_{\text{eff}} \approx 122$  keV, Table III). The composition of C-552 with impurities (463 ppm) was taken from a chemical analysis published in a previous study (Ref. 25). All statistical uncertainties on the calculations are 0.15% or less, and the uncertainties on the experimental values with the correlations removed are approximately 0.3%.

the 60 kV beam. Since EGSnrc calculations of this chamber made with pure C-552 (dashed line) did not reflect this variation, the chamber was remodeled with high- $Z$  impurities in the walls and electrode to make the chamber less air-equivalent. However, calculations of chamber response using the impure C-552 (dotted line) did not vary with air density either. Thus, since there was no statistically significant variation in the calculated results at this beam energy, the calculated data for the 60 kV beam were normalized to unity rather than to the experimental values in order to make it easier to visually distinguish differences in the respective trends. Calculations for the 100 kV beam with and without impurities were normalized to the experimental values as in Figs. 2–5, and matched experimental values to within 0.3%.

For the composition of impure C-552 used for the calculations in Fig. 6, the initial level and makeup of impurities ( $\approx 463$  ppm) were obtained from a chemical analysis of a sample of C-552 published in an earlier study of an A12 by Seuntjens *et al.*<sup>25</sup> As in that study, the modified composition of C-552 in our EGSnrc model of the A12 was tested by comparing calculated air kerma calibration coefficients ( $N_K$ ) as a function of beam effective energy with the experimental values shown in Fig. 7. Calculated  $N_K$  values in this case are defined as being proportional to the calculated  $K_{\text{air}}$  for the spectrum divided by the dose to the cavity ( $D_{\text{cav}}$ ) due to the same spectrum. These ratios were compared to experimental values by normalizing them to the value of  $N_K$  at 250 kV ( $E_{\text{eff}} \approx 122$  keV), where the effect of impurities on the absolute calculated response is the least. Figure 7 shows that the effect of impurities on the chamber response relative to the response at 250 kV ( $E_{\text{eff}} \approx 122$  keV) is significant. Increasing the amount of impurities in the simulation by 50% (to

695 ppm) brought calculated values to within 0.6% of experiment at 100 kV and above. However, calculations of the chamber response as a function of air density with this level of impurities in the C-552 plastic did not match experimental values for the 60 kV beam (Fig. 6, dotted line). The impurities also had a negligible effect on the same calculations repeated for a 100 kV beam, but this is consistent with experiment. Additional measurements and calculations at 150 kV also showed no variation, both with and without impurities included in the EGSnrc model.

In order to determine if a different composition of high- $Z$  impurities in the calculations could yield the experimental response for the A12, a hypothetical C-552 material data set was created with 695 ppm of iron ( $Z=26$ ), chosen to reflect potential contamination by machining tools. By comparison, the weighted average  $Z$  of the impurities used for the calculations in Figs. 6 and 7 is roughly 16. Calculations of the Exradin A12 response to the unfiltered 60 kV beam using the iron-doped C-552 were within 0.2% of the experimental response (data not shown). In addition, the calculated value of  $N_K$  for a 50 kV beam ( $E_{\text{eff}} \approx 23$  keV, Table III) relative to the 250 kV beam was within 0.5%. However, the agreement between the relative calculated and measured  $N_K$  values for other beams was quite poor using this wall material, exceeding 5% for the 100 kV beam ( $E_{\text{eff}} \approx 37$  keV, Table III).

## IV. DISCUSSION

The results presented in the previous section provide additional experimental evidence for the breakdown of the  $P_{TP}$  correction factor used to correct the response of non-air-equivalent chambers to low-energy x rays. Consistent with previous reports,<sup>1–3,5</sup> the extent of the breakdown is larger for lower energy x-ray spectra, and is also related to the difference between the photon cross sections of air and the material of the chamber wall and/or electrode. Overall, the experimental data were well matched by the EGSnrc Monte Carlo code, which confirms its ability to calculate ion chamber response accurately for low x-ray energies, and validates earlier predictions based on this code<sup>3</sup> provided contributions from impurities are ignored, along with approximations to the chamber geometries. Ultimately, however, the ability to model chamber response accurately at low energies is contingent on the knowledge of these factors, each of which will be discussed independently.

### IV.A. Detection of impurities and influence on chamber response

The effect of impurities on the  $P_{TP}$ -corrected chamber response as a function of the air density in the cavity was briefly investigated in our preceding paper based on Monte Carlo results.<sup>3</sup> In that study, high- $Z$  impurities were incorporated in the CAVRZnrc (Ref. 26) models of the NE 2571 and the Exradin A12, and the subsequent effect on the *ratio* of the respective calculated responses was explored (refer to Fig. 13 in that paper).<sup>3</sup> In that particular comparison, the effect of high- $Z$  impurities on the calculations was small and induced roughly the same change in the variation in response

as a function of cavity air density in both chambers. Therefore, the effect on the ratio of responses was less than 1% in that case.

In the present study, since comparisons are being made to the relative response of individual chambers, the effect of impurities on the  $P_{TP}$ -corrected response must be investigated by first determining the amount, if any, that is present. Here, it is assumed that the geometrical configurations of the chambers are sufficiently well known such that the effect of discrepancies between the actual dimensions of the chamber and our EGSnrc model is negligible. Where x-ray fluorescence measurements of chamber materials were lacking, as with the Exradin A12, the level of impurities was determined by iteratively adding suspected impurities to the material data sets of the Monte Carlo model until calculated values of  $N_K$  matched experiment. Gauging the level of impurities this way is more accurate than directly matching the calculated and measured responses as a function of pressure since  $N_K$  values have been shown to be particularly sensitive to the composition of the wall.<sup>25</sup> However, although modeling this chamber with impurities reduces discrepancies between calculated and measured  $N_K$  values, it does not prove that any impurities are present. This is supported by the inability of this Monte Carlo model to calculate the response as a function of air density (Fig. 6) using the impurity level determined from  $N_K$  data (695 ppm). The latter observation may be an indication that the Monte Carlo model must be able to accurately calculate relative  $N_K$  values in the energy range of interest in order to also accurately calculate the response as a function of air density. This notion is consistent with calculations of a hypothetical Exradin A12 chamber using iron as an impurity, where, as mentioned earlier, the relative calculated value of  $N_K$  was within 0.5% of experiment at an  $E_{\text{eff}}$  of 23 keV, and the calculated response as a function of pressure for a 60 kV beam with the same average energy was within 0.2%. Unfortunately, it was not possible to cross reference the calculated level of impurities in the A12 chamber with x-ray fluorescence spectroscopy data since this test is potentially destructive (both NE 2505/3 thimbles were damaged) and this chamber has an invaluable calibration history.

As mentioned earlier, concerns with impurities in the NE 2505/3 chambers were addressed by measuring the composition of the wall directly with x-ray fluorescence spectroscopy. Simulations of the chambers without impurities resulted in discrepancies with experiment of over 5% for the dural-walled NE 2505/3 (i.e., using pure aluminum instead of dural) and nearly 2% for the graphite thimble (normalized at  $\rho/\rho_0$  for these comparisons). For the NE 2571 and Exradin A19 chambers, x-ray fluorescence data were not obtained since experimental data were modeled well without incorporating impurities. The effect of any impurities that may be present, however, was confirmed to be negligible by comparing the calculated and measured  $N_K$  data shown in Fig. 8. For the NE 2571, the calculated  $N_K$  values normalized at 250 kV were within 1% of experiment, and the calculated results for the Exradin A19 were within 0.3%. Similarly, impur-

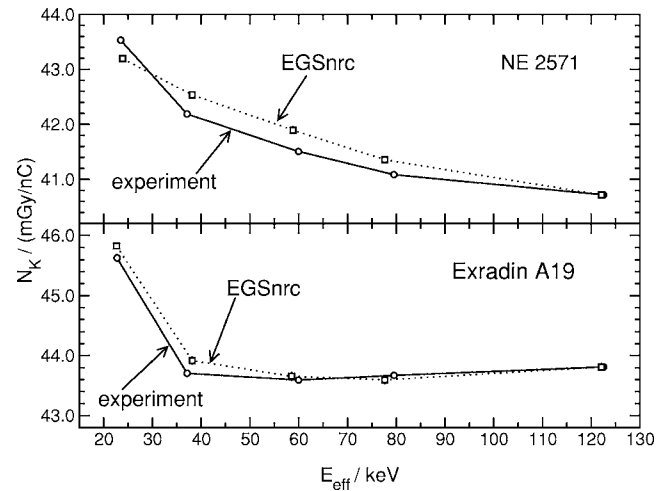


FIG. 8. As in Fig. 7 but for the NE 2571 and Exradin A19 chambers with no impurities. Statistical uncertainties on the calculations are 0.15% or less, and the uncertainties on the experimental values with the correlations removed are approximately 0.3%.

ities were presumed not to be an issue with the modified Exradin A2 chambers since none were needed to model the experimental data in Figs. 4 and 5.

For those chambers with high-Z impurities present in the walls, the effect on the relative  $P_{TP}$ -corrected response as a function of air density is, in general, more significant at low x-ray energies where the photoelectric effect dominates the total cross-section. This is due to the fact that the difference in photon cross-sections between air and high-Z materials is larger at lower x-ray energies. Exceptions to this apply to very low-energy beams (e.g.,  $\leq 30$  kV) where the effect of impurities is reduced since the contribution to the response from photon interactions in the wall is small relative to the contribution from photon interactions in the cavity.<sup>3,27,28</sup> For a given chamber and incident spectrum, however, the overall effect that impurities have on the relative chamber response will depend on the impurity type and the amount present. In short, the effect of impurities on the  $P_{TP}$ -corrected response is related to the change they induce on the photon cross-sections of the wall, and on how much electrons from the wall contribute to the response. A discussion of the influence of the wall material is provided in a preceding paper.<sup>3</sup>

#### IV.B. Sensitivity of Monte Carlo results to chamber geometry

In addition to the influence of impurities, calculations of chamber response to low-energy x rays are also sensitive to the chamber geometries defined by the EGSnrc Monte Carlo models. For instance, the calculated  $N_K$  values used to improve simulations of chamber response as a function of pressure agreed with experiment to within 1% with the exception of the value for the 50 kV beam ( $E_{\text{eff}} \approx 23$  keV) incident on the Exradin A12 with 695 ppm of impurities. The change in  $N_K$  at this energy due to impurities did not scale to the same extent it did at higher energies since a relatively large fraction of the response at this energy is due to photon interac-

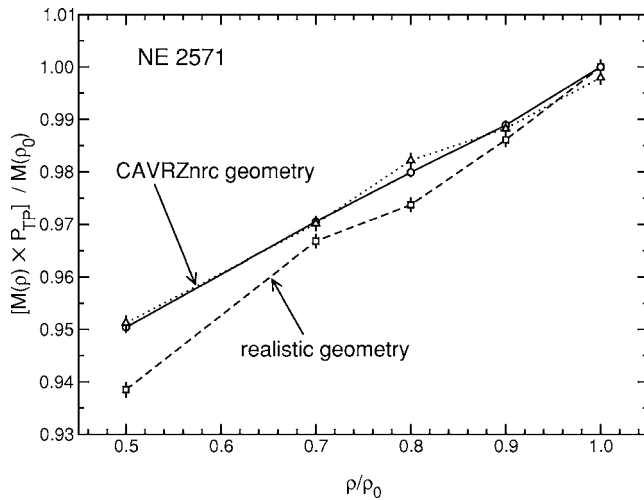


FIG. 9. Calculations of the  $P_{TP}$ -corrected response of the NE 2571 chamber free in air (no PMMA vessel) as a function of air density for two different geometrical configurations: the one used in this study, and the cylindrical one shown in Fig. 1 of our preceding paper (Ref. 3). A 40 kV PTB spectrum was used as the incident beam (see Table II of La Russa and Rogers, Ref. 3), and the solid line shows data from Fig. 3 of our preceding paper using the EGSnrc CAVRZnrc user-code (Ref. 26). The dotted line shows the same calculations using the “cavity” user code and the identical chamber geometry as that defined by CAVRZnrc. The dashed line shows the calculations of the cavity user code using a more accurate model of the chamber which includes the cone-shaped top. This latter geometry is the same as that used throughout the rest of this study for that chamber.

tions in the cavity. Instead, the remaining discrepancy in this case may be due to uncertainties associated with the dimensions of the chamber specified in our EGSnrc model. As an example, changing the cavity size may influence the response if the average range of electrons in air is on the order of the dimensions of the cavity. In this case, the average energy of an electron entering the cavity is about 25 keV, which has a CSDA range in air of  $\approx 1.2$  cm. Additionally, the chamber wall thickness may significantly influence the absolute response at this energy due to attenuation and beam hardening. Reducing the wall thickness by 15% (0.0075 cm) in our model of the A12 with impurities while keeping the outer dimensions the same reduced beam hardening by the wall and increased the cavity size. This modification is consistent with the tolerances of construction for this chamber, and brought the normalized value of  $N_K$  calculated at 50 kV to within 1.2% of the measured value relative to the value at 250 kV (data not shown). However, the reduced wall thickness had a negligible effect on the calculated response to the 60 kV beam as a function of air density. Thus, as with impurities, changes in chamber dimensions have more of an effect on values of  $N_K$  than on the response as a function of air density.

The effect of chamber dimensions was also investigated for the NE 2571. Figure 9 shows the  $P_{TP}$ -corrected response calculated for two different geometrical configurations of the NE 2571 chamber free in air (i.e., without the PMMA vessel) with the 40 kV PTB spectrum used in our preceding paper (refer to Table II).<sup>3</sup> The CAVRZnrc configuration refers to the cylindrical geometry which is also shown in Fig. 1 of that

report, and the solid-line data show the associated CAVRZnrc calculations (taken from Fig. 3). Calculations using exactly the same geometry in the “cavity” user-code are given by the dotted line and serve as a check that two user-codes give the same result. The dashed line represents calculations that included the more accurate model of the chamber used throughout this study. In this case, the  $P_{TP}$ -corrected response deviates an additional 1% below the response corresponding to reference temperature and pressure conditions. This suggests that accurately modeling the chamber dimensions is essential in order to predict the breakdown of the  $P_{TP}$  correction factor to at least within 1% at low x-ray energies. It should be noted, however, that no difference was observed in a similar comparison made between realistic (with hemispherical end) and approximated geometries of the air-equivalent Exradin A12 (without impurities).

The geometry sensitivity of these calculations for the NE 2571 has potential implications at higher energies. However, both models of the NE 2571 chamber with a  $^{60}\text{Co}$  beam showed no variation in the  $P_{TP}$ -corrected response as a function of air density (for the normal situation of a chamber with a buildup cap). This result is consistent with previous reports for different graphite-walled chambers,<sup>29–31</sup> and implies that geometrical specifications in Monte Carlo models are much less important for these types of calculations with higher-energy photons. As a check, measured values of the response to a  $^{60}\text{Co}$  beam for the NE 2571 and Exradin A12 chambers (with buildup caps) were obtained using the Co unit at NRC and showed no variation in response over the range of pressures investigated here (data not shown).

## V. CONCLUSIONS

Measurements of the response of ion chambers in a variable-pressure environment have been used to reconfirm the breakdown of the  $P_{TP}$  correction factor for low-energy x rays incident on several non-air-equivalent ion chambers. Consistent with previous reports, the breakdown is more significant at low x-ray energies where the differences between the photon cross sections of the wall materials and air are large. With the exception of one chamber, the Exradin A12, EGSnrc calculations of the relative  $P_{TP}$ -corrected response as a function of air density, and of air kerma calibration coefficients, accurately modeled experimental measurements, and aided in establishing the accuracy of this code at low x-ray energies. These calculations were also useful in detecting the presence of impurities in the materials of the chambers, particularly calculations of  $N_K$ , assuming the effect of uncertainties in the dimensions of the geometry descriptions was negligible.

It was also found that the reliability of EGSnrc in predicting the breakdown of the  $P_{TP}$  correction factor for a given chamber can be tested by comparing calculated and measured values of  $N_K$  in the energy range of interest. Values of  $N_K$  are highly sensitive to chamber dimensions and composition, and can therefore be used as a stringent test of a Monte Carlo chamber model. This is supported by the calculations of chamber response for the Exradin A12 as a func-

tion of air density, which did not match experimental measurements in the energy range where calculated and measured values of  $N_K$  were also in disagreement. Although a hypothetical model of an A12 with iron impurities was able to account for the variation in the observed response versus pressure for a 60 kV beam, subsequent calculations of  $N_K$  at higher beam energies confirmed the model to be unrealistic. Where  $N_K$  calculations were in agreement with experiment within 1%, as with the NE 2571 and Exradin A19, so too were the calculations and measurements of response as a function of air density. Thus, for those users of non-air-equivalent ion chambers in regions requiring large  $P_{TP}$  corrections, it appears the breakdown of the  $P_{TP}$  correction factor may be accurately predicted using Monte Carlo simulations provided the Monte Carlo model can accurately calculate  $N_K$  values over the energy range of interest. However, until the connection between accurate calculations of  $N_K$  and chamber response versus air density can be further validated, these predictions are best confirmed with direct experimental measurements of chamber response over a range of cavity air densities. Issues associated with the breakdown of the  $P_{TP}$  correction factor may be avoided altogether by using chambers made with air-equivalent materials known to be free of impurities.

## ACKNOWLEDGMENTS

The authors wish to thank J.E. Burns for alerting us to earlier experimental results, and Steve Davis for pointing out our use of the wrong value of  $\rho_0$  in our previous paper. The authors would also like to thank Vincent Clancy for carrying out the XRF measurements, Brian Hooten for providing us with details about the Exradin A2 and Exradin A19 chambers, and Elsayed Ali for his assistance with the calculations of x-ray spectra and associated parameters. Special appreciation goes to Hong Shen for his assistance with measurements, and for providing us with measured values of  $N_K$ . Comments from the reviewers of this manuscript were also very helpful and appreciated. This research was enabled by support from the Natural Sciences and Engineering Research Council of Canada (NSERC) and the Canada Research Chairs program.

<sup>a)</sup>Electronic mail: dlarussa@physics.carleton.ca

<sup>b)</sup>Electronic mail: drogers@physics.carleton.ca

<sup>1</sup>S. L. Griffin, L. A. DeWerd, J. A. Micka, and T. D. Bohm, "The effect of ambient pressure on well chamber response: Experimental results with empirical correction factors," *Med. Phys.* **32**, 700–709 (2005).

<sup>2</sup>T. D. Bohm, S. L. Griffin, J. P. M. DeLuca, and L. A. DeWerd, "The effect of ambient pressure on well chamber response: Monte Carlo calculated results for the HDR 1000 Plus," *Med. Phys.* **32**, 1103–1114 (2005).

<sup>3</sup>D. J. La Russa and D. W. O. Rogers, "An EGSnrc investigation of the  $P_{TP}$  correction factor for ion chambers in kilovoltage x-rays," *Med. Phys.* **33**, 4590–4599 (2006).

<sup>4</sup>W. Will and A. Rakow, "Measuring of the standard ionic dose in compact and liquid media during x-ray and gamma irradiation by energies between 50 keV and 3 MeV," *Strahlentherapie* **141**, 166–175 (1971) [English translation in *Rad. Sci. Trans.* **8** (1973)].

<sup>5</sup>J. E. Burns and D. H. Pritchard, Technical Report Rad. Sci. 40, National Physical Laboratory, Teddington, U.K., 1977.

<sup>6</sup>F. H. Attix, *Introduction to Radiological Physics and Radiation Dosimetry* (Wiley, New York, 1986).

<sup>7</sup>A. E. Nahum, W. H. Henry, and C. K. Ross, "Response of carbon and aluminium walled thimble chamber in <sup>60</sup>Co and 20 MeV electron beams," in Proceedings of VII International Conference on Medical Physics, *Med. Biol. Eng. Comput.* **23**, 612–613 (1985).

<sup>8</sup>L. A. Buckley, I. Kawrakow, and D. W. O. Rogers, "An EGSnrc investigation of cavity theory for ion chambers measuring air kerma," *Med. Phys.* **30**, 1211–1218 (2003).

<sup>9</sup>J. P. McCaffrey, B. Downton, H. Shen, D. Niven, and M. McEwen, "Perradiation effects on ionization chambers used in radiation therapy," *Phys. Med. Biol.* **50**, N121–N133 (2005).

<sup>10</sup>D. W. O. Rogers, B. A. Faddegon, G. X. Ding, C.-M. Ma, J. Wei, and T. R. Mackie, "BEAM: A Monte Carlo code to simulate radiotherapy treatment units," *Med. Phys.* **22**, 503–524 (1995).

<sup>11</sup>E. Mainegra-Hing and I. Kawrakow, "Efficient x-ray tube simulations," *Med. Phys.* **33**, 2683–2690 (2006).

<sup>12</sup>E. S. M. Ali and D. W. O. Rogers, "Efficiency improvements of x-ray simulations in EGSnrc user-codes using Bremsstrahlung Cross Section Enhancement (BCSE)," *Med. Phys.* **34**, 2143–2154 (2007).

<sup>13</sup>K. Cranley, B. J. Gilmore, G. W. Fogarty, and L. Desponds, Catalogue of diagnostic x-ray spectra and other data, CD edition 1997, electronic version prepared by D. Sutton, Technical Report 78, The Institute of Physics and Engineering in Medicine (IPEM), York, 1997.

<sup>14</sup>R. Birch and M. Marshall, "Computation of Bremsstrahlung x-ray spectra and comparison with spectra measured with a Ge(Li) detector," *Phys. Med. Biol.* **24**, 505–517 (1979).

<sup>15</sup>F. Verhaegen, A. E. Nahum, S. Van de Putte, and Y. Namito, "Monte Carlo modelling of radiotherapy kV x-ray units," *Phys. Med. Biol.* **44**, 1767–1789 (1999).

<sup>16</sup>M. R. Ay, M. Shahriari, S. Sarkar, M. Adib, and H. Zaidi, "Monte Carlo simulation of x-ray spectra in diagnostic radiology and mammography using MCNP4C," *Phys. Med. Biol.* **49**, 4897–4917 (2004).

<sup>17</sup>G. Ullman, M. Sandborg, D. R. Dance, M. Yaffe, and G. A. Carlsson, "A search for optimal x-ray spectra in iodine contrast media mammography," *Phys. Med. Biol.* **50**, 3143–3152 (2005).

<sup>18</sup>ISO, *Guide to the Expression of Uncertainties in Measurement* (International Organisation for Standardization, Geneva, Switzerland, 1993).

<sup>19</sup>R. E. Bentley, *Uncertainty in Measurement: The ISO Guide* (National Measurement Laboratory CSIRO, Australia, 2003).

<sup>20</sup>I. Kawrakow, "Accurate condensed history Monte Carlo simulation of electron transport. I. EGSnrc, the new EGS4 version," *Med. Phys.* **27**, 485–498 (2000).

<sup>21</sup>I. Kawrakow and D. W. O. Rogers, The EGSnrc Code System: Monte Carlo simulation of electron and photon transport, Technical Report PIRS-701, National Research Council of Canada, Ottawa, Canada (2000); See <http://www.irs.inms.nrc.ca/inms/irs/EGSnrc/EGSnrc.html>

<sup>22</sup>I. Kawrakow, E. Mainegra-Hing, and D. W. O. Rogers, EGSnrcMP: The multi-platform environment for EGSnrc, Technical Report PIRS-877, National Research Council of Canada, Ottawa, Canada, 2003.

<sup>23</sup>I. Kawrakow, egsp: The EGSnrc C++ class library, Technical Report PIRS-899, National Research Council of Canada, Ottawa, Canada, 2005.

<sup>24</sup>M. J. Rivard, B. M. Coursey, L. A. DeWerd, M. S. Huq, G. S. Ibbott, M. G. Mitch, R. Nath, and J. F. Williamson, "Update of AAPM Task Group No.43 Report: A revised AAPM protocol for brachytherapy dose calculations," *Med. Phys.* **31**, 633–674 (2004).

<sup>25</sup>J. P. Seuntjens, I. Kawrakow, J. Borg, F. Hobeila, and D. W. O. Rogers, in *Recent Developments in Accurate Radiation Dosimetry, Proceedings of an International Workshop*, edited by J. P. Seuntjens and P. Mobit (Medical Physics, Madison, WI, 2002), pp. 69–84.

<sup>26</sup>D. W. O. Rogers, I. Kawrakow, J. P. Seuntjens, and B. R. B. Walters, NRC User Codes for EGSnrc, Technical Report PIRS-702, National Research Council of Canada, Ottawa, Canada (2000); See <http://www.irs.inms.nrc.ca/inms/irs/EGSnrc/EGSnrc.html>

<sup>27</sup>C.-M. Ma and A. E. Nahum, "Bragg-Gray theory and ion chamber dosimetry for photon beams," *Phys. Med. Biol.* **36**, 413–428 (1991).

<sup>28</sup>J. Borg, I. Kawrakow, D. W. O. Rogers, and J. P. Seuntjens, "Monte Carlo study of correction factors for Spencer-Attix cavity theory at photon energies at or above 100 keV," *Med. Phys.* **27**, 1804–1813 (2000).

<sup>29</sup>D. V. Cormack and H. E. Johns, "The measurement of high-energy radiation intensity," *Radiat. Res.* **1**, 133–157 (1954).

<sup>30</sup>G. N. Whyte, "Measurement of the Bragg-Gray stopping power correction," *Radiat. Res.* **6**, 371–379 (1957).

<sup>31</sup>F. H. Attix, L. DeLa Vergne, and V. H. Ritz, "Cavity ionization as a function of wall material," *J. Res. Natl. Bur. Stand.* **60**, 235–243 (1958).